LEVEL II

COMPUTER SCIENCE
TECHNICAL REPORT SERIES

UNIVERSITY OF MARYLAND
COLLEGE PARK, MARYLAND
20742

Accession For
NTIS GRA&I
DDC TAB
Unannounced
Justification
By
Distribution/
Availability Codes
Dist | Avail and/or special
A

(14) CSC-TR-694
DAAG53-76C-0138

(11) September, 1978

(6) STRAIGHT EDGE ENHANCEMENT AND MAPPING,

(12) 15

(10) Shmuel Peleg
Azriel Rosenfeld
Computer Science Center
University of Maryland
College Park, MD 20742

ABSTRACT

An iterative reinforcement scheme is used to enhance straight portions of edges in an image and to obtain refined estimates of their slopes. This makes it much easier to detect significant straight edge segments in the image and thus to map the image's straight edge content.

(15)

The support of the Defense Advanced Research Projects Agency and the U.S. Army Night Vision Laboratory under Contract DAAG53-76C-0138, DARPA Order-3206) is gratefully acknowledged, as is the help of Ms. Kathryn Riley in preparing this paper.

403 018

1. Introduction

There are a number of standard methods of detecting straight edges (or lines) in an image. One of the most commonly used of these is the Hough transform, in which, for each edge point P, we estimate the slope and distance from the origin of the straight line through P. In this way, the edge points are mapped into points in (slope, distance) space. Evidently, sets of collinear edge points map into approximately the same point in this "Hough space"; thus we can detect straight edges, whether continuous or broken, by looking for high concentrations of points in Hough space. For a recent review on "Hough transforms" see [1].

A problem that arises in the use of Hough transforms is the uncertainty in estimating the slopes of the edge points. When a standard edge detector, based on 3x3 neighborhoods, is used, these slopes are quite uncertain. Moreover, this leads to an even greater uncertainty in estimating distance if the given edge point is far away from the point where the line through it comes closest to the origin.

The usefulness of the Hough transform can be improved by increasing the accuracy of the edge slope estimates. This can be done using an iterative process analogous to those described in [2] and [3-4], where the slope and magnitude of edge (or line) responses are iteratively reestimated at each point based on the values of the current estimates at nearby points. The enhanced edge points can then be grouped into connected components of points having essentially the same slope; averaging the slope estimates over these components further increases their accuracy.

Section 2 describes the enhancement process, and gives examples of its application to extracting straight edge segments from aerial photography. The high quality of these segments in turn facilitates the construction of a map representing the straight edges in the image and their relationships, as illustrated in Section 3.

2. Straight edge enhancement

Initially, the edge magnitude and direction at each point are estimated using the standard Sobel edge detector. In the neighborhood $\begin{matrix} a & b & c \\ d & e & f \\ g & h & i \end{matrix}$, this is defined as having magnitude $\sqrt{\Delta_x^2 + \Delta_y^2}$ and direction $\tan^{-1}(\Delta_x/\Delta_y)$*, where

$$\Delta_x = c+2f+i-a-2d-g$$

$$\Delta_y = a+2b+c-g-2h-i$$

For each neighbor Q of P, let M_Q and D_Q be the magnitude and direction of the edge response at Q; let D_P be the direction of the edge response at P, and let D be the direction of the line joining P to Q. Then the degree to which the response at Q supports that at P is

$$S_Q \equiv M_Q \cos(D_Q - D)\cos(D_P - D) \tag{1}$$

Note that this is a maximum when D_Q and D_P are both collinear with D, which is intuitively reasonable.

Using (1), we compute new estimates of the magnitude and direction of the edge at P as follows:

a) The new magnitude is proportional to ΣS_Q, where the sum is taken over all the neighbors Q of P. (Note that this does not depend directly on the previous estimate of P itself.)

b) The new direction is basically the direction to that neighbor Q_i for which S_Q is greatest, but modified as follows: Let the direction to Q_i be 45i°. Then the

---

* The direction of the edge is perpendicular to the gradient.

responses at Q_{i+1} and Q_{i+5} tend to bias the direction toward an angle greater than $45i°$, while the responses at Q_{i-1} and Q_{i+3} tend to bias it toward a smaller angle. The final direction estimate is thus

$$45i° + \frac{S_{i+1} + S_{i+5}}{S} 22\frac{1}{2}° - \frac{S_{i-1} + S_{i+3}}{S} 22\frac{1}{2}°$$

where S_j is short for S_{Q_j}, and $S=S_{i-1}+S_i+S_{i+1}+S_{i+3}+S_{i+4}+S_{i+5}$.

Note that this ignores the sense of the edge (i.e., which side is light and which dark); this remains the same as in the previous estimate.

c) We set the magnitude to zero unless **one** of the following conditions is met: Let Q_1, Q_2, Q_3 be the points at which the response magnitude is highest, second highest, and third highest, respectively. Then we require that Q_1 be opposite Q_2, Q_2 be opposite Q_3, or Q_3 be opposite Q_1. These conditions correspond to the fact that for a straight edge, the response magnitude should be maximum for a pair of opposite directions.

This entire process can be iterated to further reinforce the responses.

Figure 1 shows an aerial photograph of an airport (a), the initial edge response magnitudes (b), and the results of three iterations of the reinforcement process (c-e). Figure 2 shows analogous results for another airport photograph, taken from a higher altitude. The enhancement effects are quite apparent.

3. Straight edge mapping

The enhanced edge points are now grouped into connected components of points having essentially the same slope. This is done as follows: The picture (after edge enhancement) is scanned row by row. On each row, we examine the points having above-threshold edge magnitudes. For each row of such points, we compute a running average of slopes, and accept a point into the run only if its slope is very close to the current average. This yields runs of points all having approximately the same slope. Adjacent runs on consecutive rows are linked if their averages are very close to one another. In this way, we can assign distinguished labels to connected components of edge points that have above-threshold magnitudes and very similar slopes. Components having very few points are discarded. The thresholds used to define acceptable edge magnitudes, slope differences, and component sizes were quite low (9 gray levels, 0.2 radians, and 8 pixels, in our experiments).

The components obtained in this way are all essentially straight line segments. For each such segment s, we tabulate the average slope of s; the distance of the straight line ℓ containing s from the origin; and the distances of s's end-points, along ℓ, from the point of closest approach to the origin. These quantities are given in Table 1 for the picture in Figure 1. A printout of the components, labelled 0,1,...,9, A,...,Z,0,1,..., is shown in Figure 3.

The components can now be linked into sets that are (almost exactly) collinear or that meet (approximately) at a common endpoint. A list of such connections, for the components of Table 1, is given in Table 2. The linked components can now form the basis for an interpretation of the straight line content of the given picture. This process of interpretation will be the subject of a subsequent report.

References

1. S. D. Shapiro, Feature space transforms for curve detection, Pattern Recognition 10, 1978, 129-143.

2. G. J. VanderBrug, Experiments in iterative enhancement of linear features, Computer Graphics and Image Processing 6, 1977, 25-42.

3. S. W. Zucker, R. A. Hummel, and A. Rosenfeld, An application of relaxation labelling to line and curve enhancement, IEEE Trans. on Computers 26, 1977, 394-403 and 922-929.

4. B. J. Schachter, A. Lev, S. W. Zucker, and A. Rosenfeld, An application of relaxation methods to edge reinforcement, IEEE Trans. on Systems, Man, and Cybernetics 7, 1977, 813-816.

Best
Available
Copy

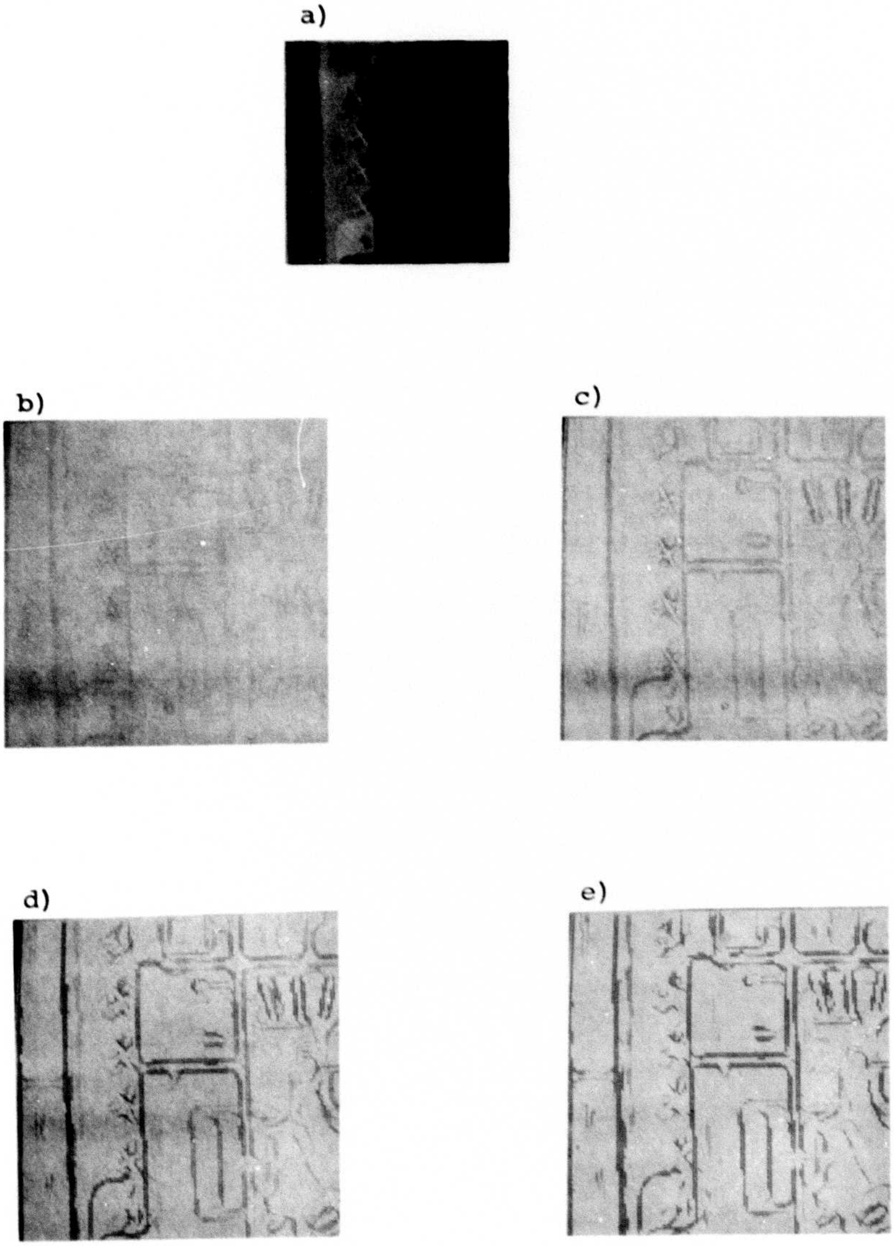

Figure 1. a. Aerial photograph of an airport
b. Initial edge response
c-e. Results of three iterations of the reinforcement process

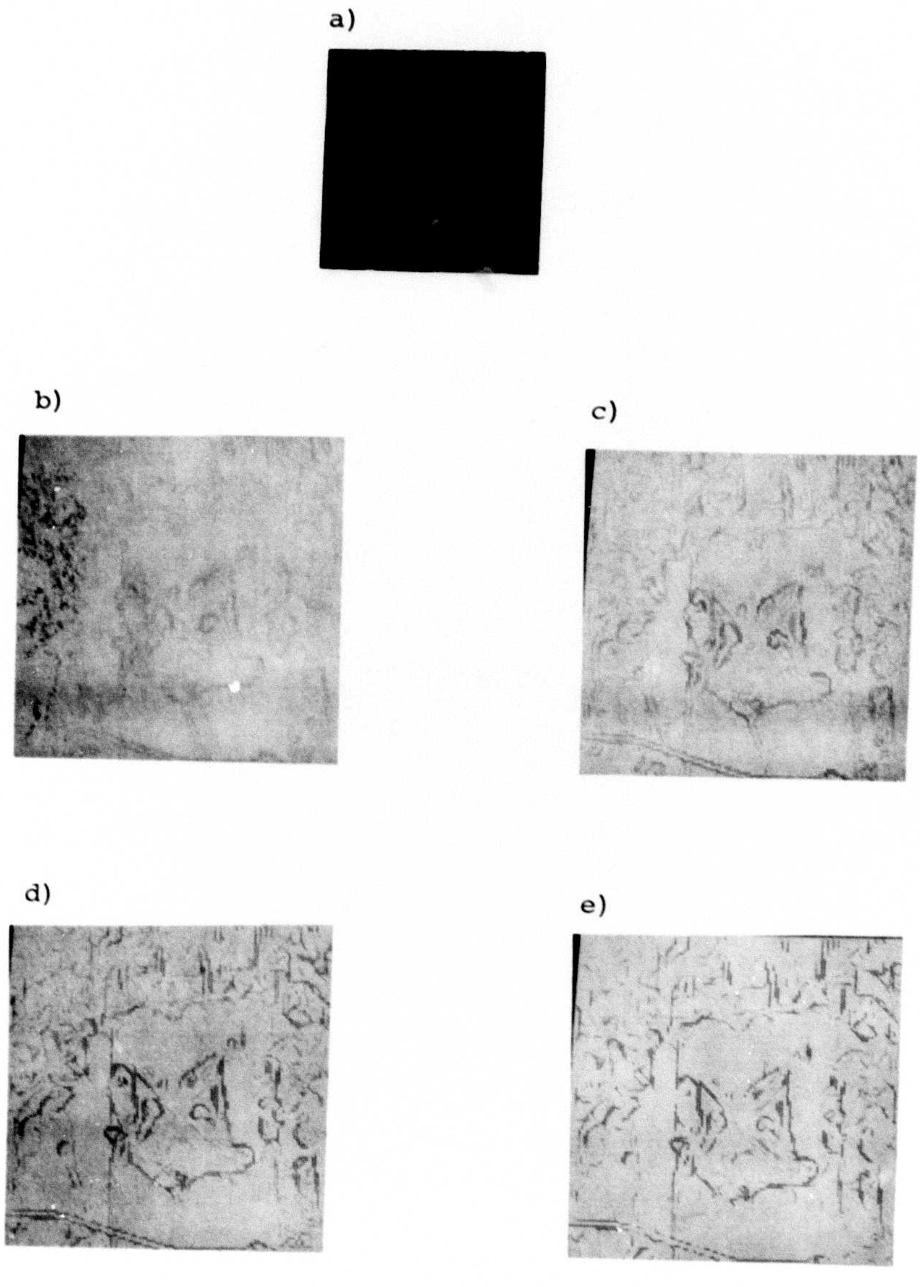

Figure 2. a. Aerial photograph of an airport
b. Initial edge response
c-e. Results of three iterations of the reinforcement process

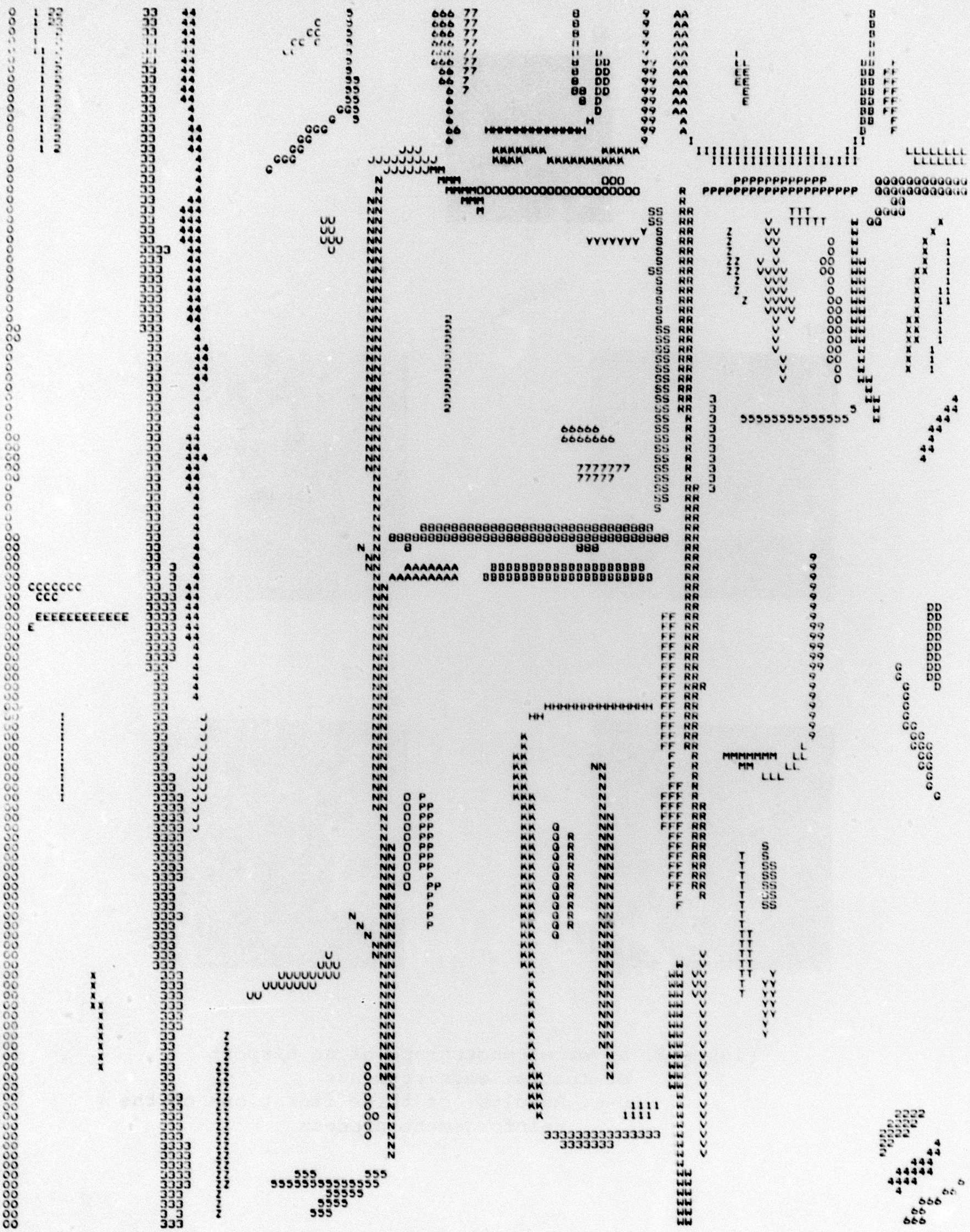

Figure 3. Connected components of edge points for Figure 1.

A	B	C	D	E	F	G	H
1	0	157.180	3.440	1.996	123.997	(4,129)	(3,3)
2	1	475.187	-11.308	-123.666	-109.638	(6,3)	(7,17)
3	2	160.000	12.317	109.690	123.714	(9,17)	(8,3)
4	3	472.493	-23.167	-123.748	-1.696	(20,3)	(25,129)
5	4	158.743	27.990	54.543	123.567	(27,72)	(25,3)
6	5	471.600	-46.799	-123.833	-112.830	(46,3)	(47,14)
7	6	163.414	65.798	107.043	120.143	(55,16)	(57,3)
8	7	466.962	-55.740	-126.763	-118.725	(62,3)	(61,11)
9	8	163.727	82.933	109.698	118.744	(76,12)	(75,3)
10	9	469.136	-81.890	-125.739	-112.742	(84,3)	(84,16)
11	A	160.083	92.059	109.277	121.301	(89,15)	(88,3)
12	B	467.900	-108.621	-127.703	-115.676	(113,3)	(112,15)
13	C	92.250	-41.031	118.999	123.406	(38,7)	(42,4)
14	D	192.909	73.410	117.153	123.148	(78,13)	(78,7)
15	E	168.444	109.276	103.258	108.339	(97,12)	(96,7)
16	F	158.077	116.763	110.838	117.837	(116,15)	(116,8)
17	G	363.900	78.443	-94.507	-82.858	(46,13)	(36,19)
18	H	6.571	-107.200	71.217	84.254	(64,15)	(77,14)
19	I	318.800	104.787	-117.029	-95.092	(112,16)	(90,16)
20	J	3.000	-107.185	52.247	60.244	(49,18)	(57,18)
21	K	317.654	106.825	-86.793	-68.769	(83,17)	(65,18)
22	L	310.533	113.874	-120.966	-113.939	(125,18)	(118,17)
23	M	581.154	-121.930	1.707	8.869	(57,19)	(63,23)
24	N	161.989	53.219	6.437	104.417	(52,118)	(50,20)
25	O	627.083	-107.029	61.686	81.684	(63,21)	(83,21)
26	P	627.812	-106.887	91.462	110.462	(92,21)	(111,21)
27	Q	3.875	-101.207	116.905	129.051	(113,24)	(125,20)
28	R	158.861	91.550	33.355	104.397	(92,92)	(89,21)
29	S	474.442	-89.057	-101.224	-71.208	(85,23)	(86,53)
30	T	609.500	-121.123	81.726	85.842	(103,23)	(107,24)
31	U	66.875	-92.609	96.358	98.383	(43,26)	(44,24)
32	V	179.206	119.618	62.494	78.543	(102,40)	(100,24)
33	W	166.687	120.293	71.681	91.877	(114,44)	(111,24)
34	X	452.150	-98.942	-124.276	-108.790	(122,24)	(118,39)
35	Y	326.250	90.677	-95.689	-88.620	(84,25)	(77,26)
36	Z	488.600	-111.178	-84.096	-76.816	(95,25)	(97,32)
37	0	475.629	-112.300	-96.167	-82.137	(108,26)	(109,40)
38	1	144.687	109.616	102.281	115.429	(121,39)	(123,26)
39	2	472.100	-59.760	-92.489	-83.489	(59,34)	(59,43)
40	3	474.100	-95.265	-82.305	-73.308	(93,42)	(93,51)
41	4	412.909	-96.937	-139.242	-132.031	(124,42)	(120,48)
42	5	133	-82.928	97.111	111.112	(97,44)	(111,43)
43	6	318.900	78.017	-83.440	-77.445	(80,46)	(74,46)
44	7	3.750	-74.583	78.833	84.867	(76,50)	(82,49)
45	8	313.657	71.722	-86.642	-51.643	(87,56)	(52,56)
46	9	155.792	105.427	52.361	70.360	(106,76)	(106,58)
47	A	2.188	-66.187	53.493	61.473	(52,60)	(60,59)
48	B	1.833	-66.099	65.218	86.214	(64,60)	(85,60)
49	C	310.600	65.968	-9.644	-3.648	(12,61)	(6,61)
50	D	159.412	122.901	53.140	61.161	(122,71)	(121,63)
51	E	2.462	-62.609	7.524	19.545	(6,65)	(18,64)
52	F	473.881	-89.170	-60.679	-31.637	(87,64)	(89,93)
53	G	500.500	-129.050	-21.786	-7.896	(117,69)	(122,82)
54	H	320.312	49.007	-88.160	-73.127	(85,73)	(70,74)
55	I	472.778	-10.793	-52.840	-44.841	(10,74)	(10,82)
56	J	154.412	26.256	42.705	53.728	(27,85)	(28,74)
57	K	472.970	-70.128	-49.798	-11.769	(69,76)	(71,114)
58	L	60.375	18.859	109.005	114.824	(100,80)	(105,77)
59	M	311.889	90.987	-99.862	-93.863	(101,78)	(95,78)
60	N	160.193	80.425	14.502	45.549	(80,110)	(78,79)
61	O	472.900	-54.665	-44.097	-35.098	(54,82)	(54,91)
62	P	162.227	98.623	29.025	42.059	(57,95)	(56,82)
63	Q	471.000	-72.913	-42.174	-31.174	(73,85)	(73,96)
64	R	157.000	74.971	32.060	41.060	(75,95)	(75,86)
65	S	162.750	102.329	28.221	34.268	(101,93)	(100,87)
66	T	470.800	-97.112	-39.425	-25.426	(97,88)	(97,102)
67	U	330.571	19.742	-48.970	-37.628	(45,99)	(34,102)
68	V	159.000	92.240	7.232	27.228	(92,118)	(92,98)
69	W	473.267	-89.159	-26.190	-.175	(89,99)	(90,125)
70	X	485.364	-17.677	-24.760	-15.709	(14,100)	(15,109)
71	Y	146.818	97.449	31.133	37.204	(100,106)	(101,100)
72	Z	468.031	-30.099	-21.983	-3.961	(31,106)	(30,124)
73	0	473.000	-49.356	-17.134	-10.135	(49,109)	(49,116)
74	1	320.875	7.833	-86.746	-82.688	(86,113)	(82,114)
75	2	383.467	-65.922	-100.620	-94.218	(120,114)	(115,118)
76	3	773	-10.076	72.083	86.082	(72,116)	(86,116)
77	4	47.437	47.993	109.932	113.096	(116,121)	(122,117)
78	5	20.875	3.809	37.440	51.343	(37,121)	(51,120)
79	6	362.364	-52.873	-113.938	-105.481	(125,121)	(118,125)

Table 1. Properties of straight edge components extracted from Fig 1.
A: Component number
B: Representation of component in Figure 3.
C: Slope (radians x 100)
D: Distance of the line containing the segment from origin
E,F: Positions of the segment endpoints on the line
(measured from the foot of perpendicular from origin to line)
G,H: Coordinates of segment endpoints

All distances are measured in units of pixels

CONNECT	6	TO	20	BY	RIGHT ANGLE
CONNECT	8	TO	18	BY	RIGHT ANGLE
CONNECT	10	TO	21	BY	RIGHT ANGLE
CONNECT	12	TO	19	BY	RIGHT ANGLE
CONNECT	18	TO	14	BY	RIGHT ANGLE
CONNECT	19	TO	11	BY	RIGHT ANGLE
CONNECT	20	TO	7	BY	RIGHT ANGLE
CONNECT	22	TO	16	BY	RIGHT ANGLE
CONNECT	25	TO	29	BY	RIGHT ANGLE
CONNECT	26	TO	37	BY	RIGHT ANGLE
CONNECT	27	TO	34	BY	RIGHT ANGLE
CONNECT	28	TO	26	BY	RIGHT ANGLE
CONNECT	29	TO	45	BY	RIGHT ANGLE
CONNECT	32	TO	30	BY	RIGHT ANGLE
CONNECT	33	TO	27	BY	RIGHT ANGLE
CONNECT	42	TO	33	BY	RIGHT ANGLE
CONNECT	48	TO	52	BY	RIGHT ANGLE
CONNECT	54	TO	57	BY	RIGHT ANGLE
CONNECT	57	TO	76	BY	RIGHT ANGLE
CONNECT	67	TO	72	BY	RIGHT ANGLE
CONNECT	74	TO	60	BY	RIGHT ANGLE
CONNECT	76	TO	68	BY	RIGHT ANGLE
CONNECT	78	TO	24	BY	RIGHT ANGLE
CONNECT	47	TO	48	BY	CONTINUATION
CONNECT	52	TO	69	BY	CONTINUATION
CONNECT	56	TO	5	BY	CONTINUATION
CONNECT	68	TO	28	BY	CONTINUATION

Table 2. List of connections for the components in Table 1.

UNCLASSIFIED

SECURITY CLASSIFICATION OF THIS PAGE (When Data Entered)

REPORT DOCUMENTATION PAGE

READ INSTRUCTIONS BEFORE COMPLETING FORM

1. REPORT NUMBER	2. GOVT ACCESSION NO.	3. RECIPIENT'S CATALOG NUMBER
4. TITLE (and Subtitle) STRAIGHT EDGE ENHANCEMENT AND MAPPING		5. TYPE OF REPORT & PERIOD COVERED Technical Report
		6. PERFORMING ORG. REPORT NUMBER TR-694
7. AUTHOR(s) Shmuel Peleg		8. CONTRACT OR GRANT NUMBER(s) DAAG53-76C-0138
9. PERFORMING ORGANIZATION NAME AND ADDRESS University of Maryland Computer Science Center College Park, MD 20742		10. PROGRAM ELEMENT, PROJECT, TASK AREA & WORK UNIT NUMBERS
11. CONTROLLING OFFICE NAME AND ADDRESS U.S. Army Night Vision Lab. Ft. Belvoir, VA 22060		12. REPORT DATE September 1978
		13. NUMBER OF PAGES 13
14. MONITORING AGENCY NAME & ADDRESS (if different from Controlling Office)		15. SECURITY CLASS. (of this report) UNCLASSIFIED
		15a. DECLASSIFICATION/DOWNGRADING SCHEDULE

16. DISTRIBUTION STATEMENT (of this Report)

Approved for public release; distribution unlimited.

17. DISTRIBUTION STATEMENT (of the abstract entered in Block 20, if different from Report)

18. SUPPLEMENTARY NOTES

19. KEY WORDS (Continue on reverse side if necessary and identify by block number)

Pattern recognition
Image processing
Edge detection
Line detection

20. ABSTRACT (Continue on reverse side if necessary and identify by block number)

An iterative reinforcement scheme is used to enhance straight portions of edges in an image and to obtain refined estimates of their slopes. This makes it much easier to detect significant straight edge segments in the image and thus to map the image's straight edge content.

DD FORM 1 JAN 73 1473 EDITION OF 1 NOV 65 IS OBSOLETE

UNCLASSIFIED

SECURITY CLASSIFICATION OF THIS PAGE (When Data Entered)